Beam Application to Nanotechnology based on Subpicosecond Pulse Radiolysis

Seiichi Tagawa

The Institute of Scientific and Industrial Research, Osaka University
8-1 Mihogaoka, Ibaraki, Osaka 567-0047, Japan

Acknowledgment

- Coworkers
- T. Kozawa
- A. Saeki
- H. Yamamoto
- K. Okamoto
- Prof. S. Seki
- Tsukuda

New Sub-picosecond Pulse Radiolysis System

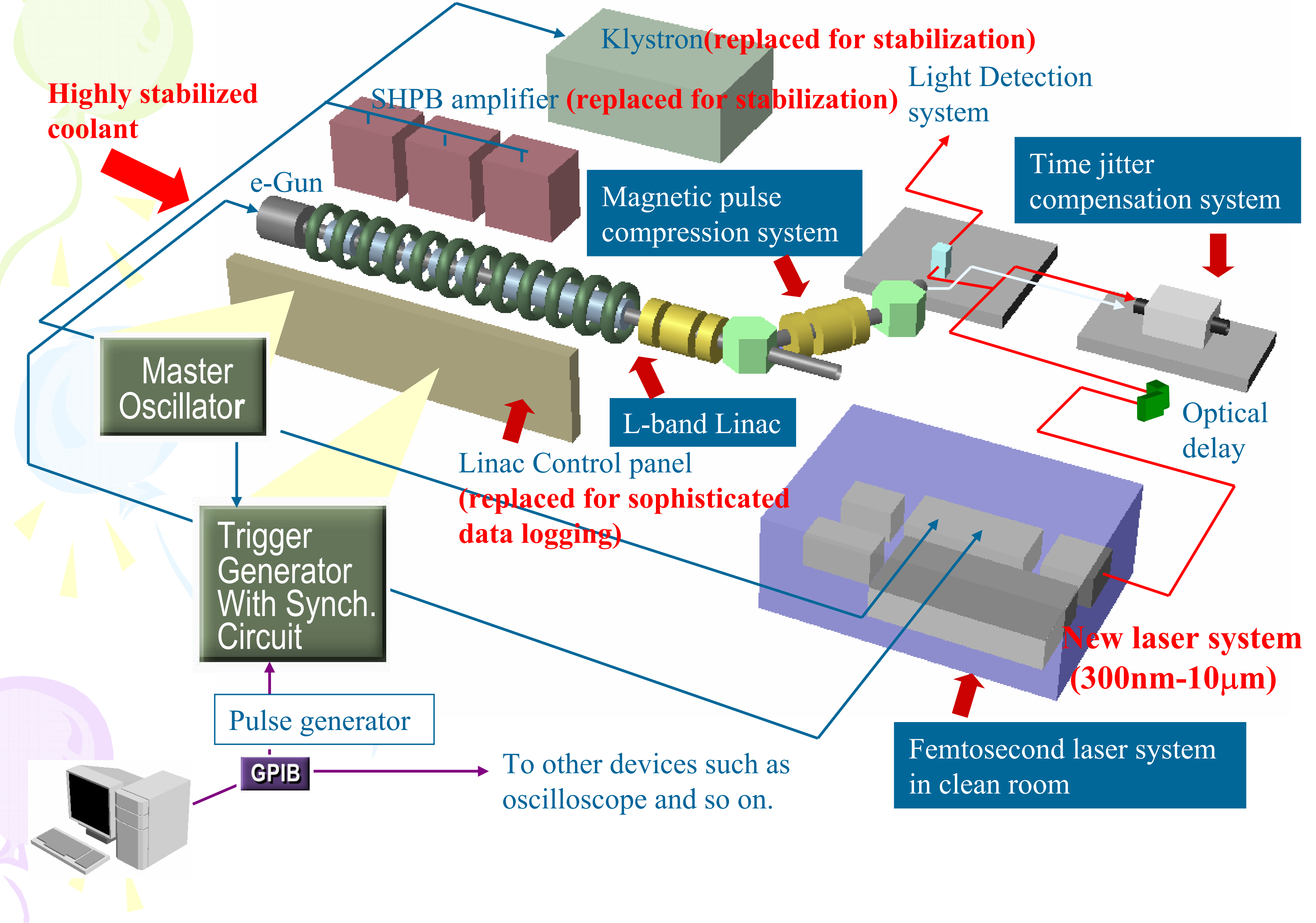

New Femtosecond Pulse Radiolysis System

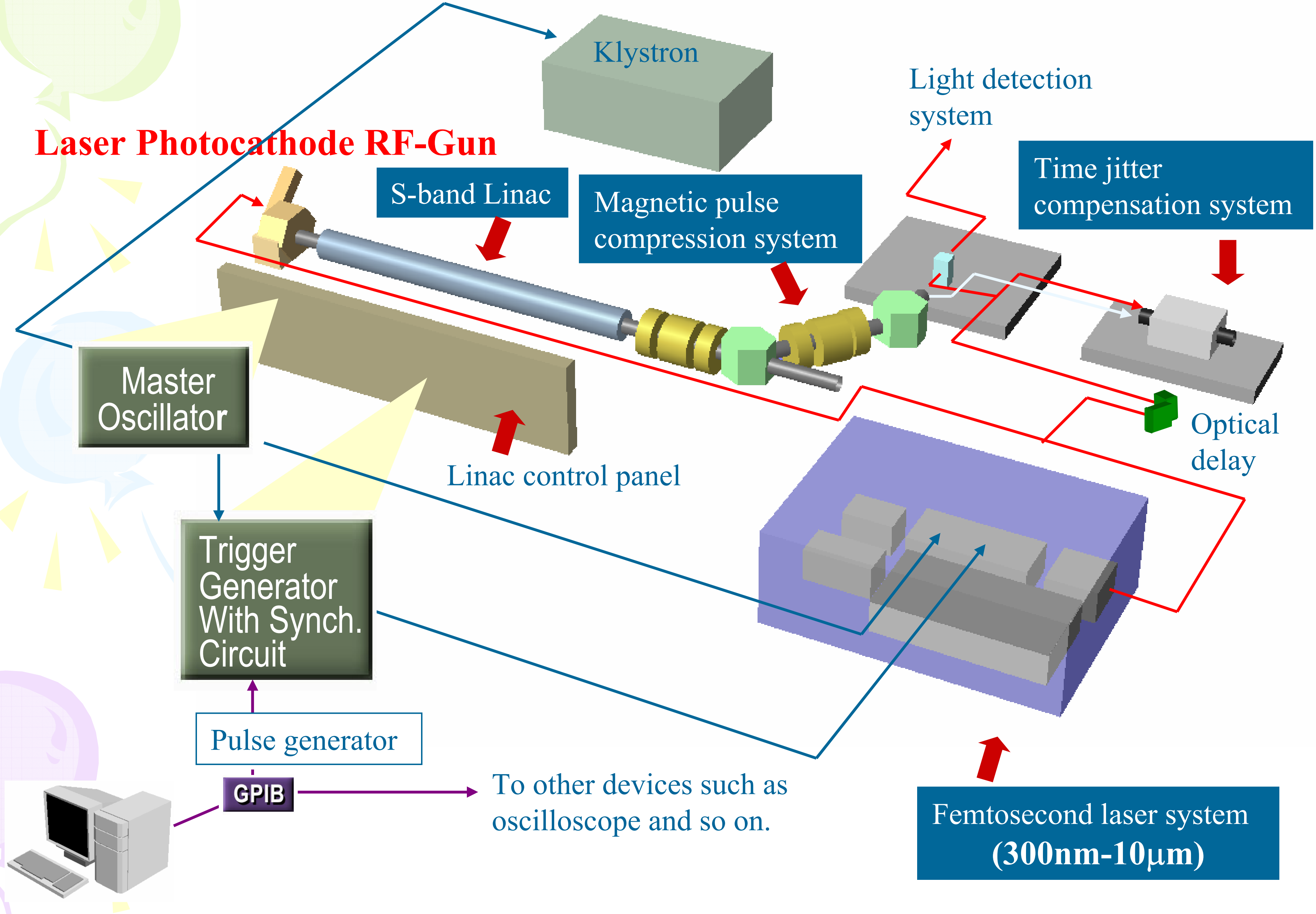

Co-operation of Our Research Groups in The Institute of Scientific and Industrial Research, Osaka University

Department of Beam Science & Technology
(S. Tagawa, Y.Yamamoto, K.Kobayashi, A.Saeki)

Department of Beam Processing for Nanotechnology
(S.Tagawa, T.Kozawa, S.Seki)

Radiation Laboratory
20 Members
(S.Tagawa, Y.Yamamoto, T.Kozawa, S.Seki, K.Kobayashi, A.Saeki from our group)

Nanofoundry
Y.Matsui and K.Okamoto
in Tight Co-operation with
S.Tagawa, T.Kozawa, S.Seki

21st Century COE Program
Chairman of 21st Century COE Program Committee （S. Tagawa）
5 Research Groups:IT Nanotechnology G (Group Leader：S.Tagawa)

Nanofabrication Research of Our Group Based on Radiation Chemistry

Top-down Type Nanotechnology
Nanolithographies

Bottom-up Type Nanotechnology
Material Design and synthesis

Beam Science and Technology

Research Consortiums
SELETE(ASUKA) :
EB,F2,Immersion ArF
ASET : EUV
Several Companies

Combination of Two Nanotechnologies
Mass-production Type Nanofabrication

Next Generation Lithograpy and Future Lithographies <30nm
(CD control <2nm)
(So-called Mass Production Type)

Nanoscience and Nanotechnology
(So-called Non-Mass Production Type)

Nanobeam Processes and Development of Nanomaterials

Ultra-fine Electron Beam atternP

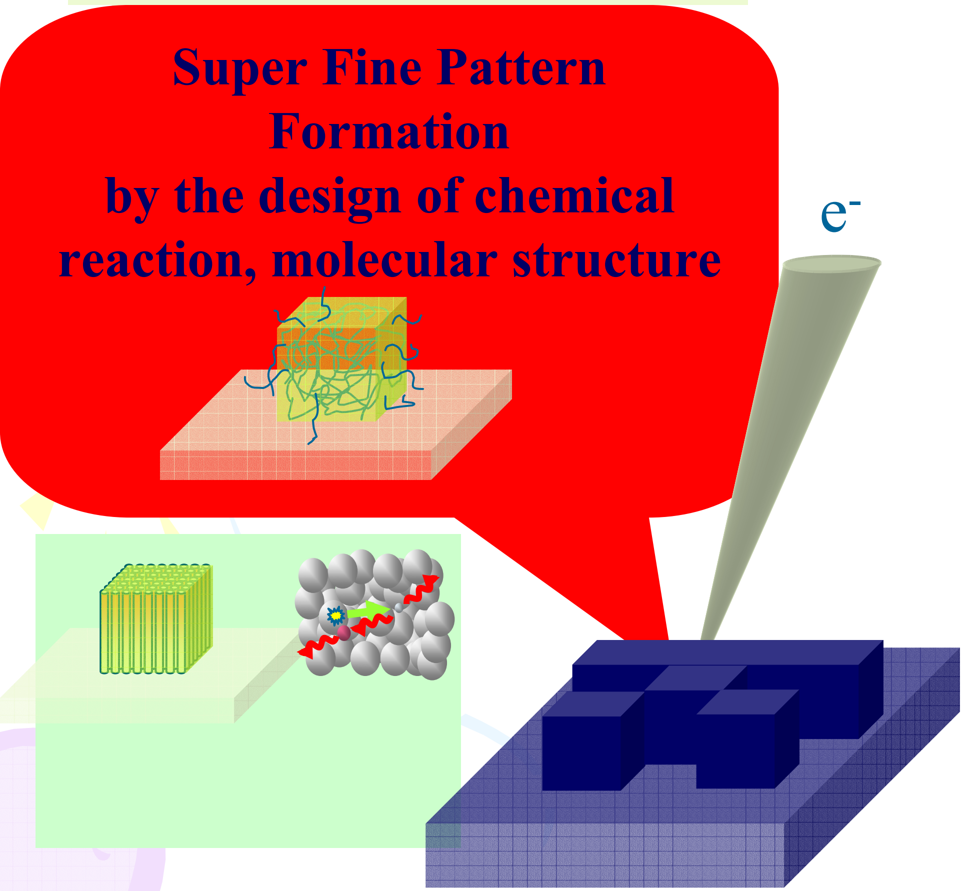

Use of Single Charged Particle Events

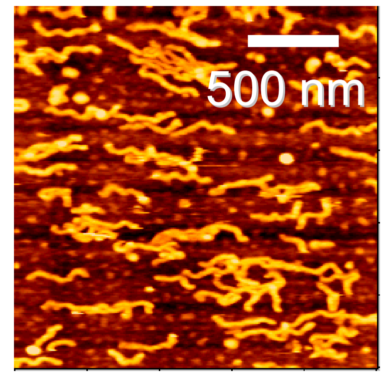

Nano-fluorescent Light

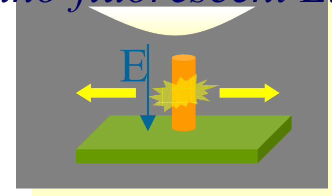

Single Ion Track

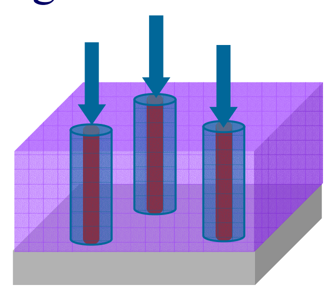

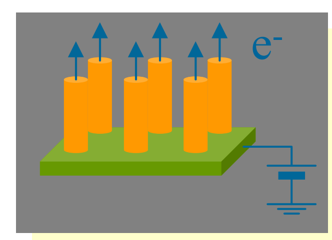

Field Emitter

Nano Materials

C60 etc., Carbon Nanotubes → 1985, 1991 Iijima

Size Control, Spatial Distribution, Structure, etc.

Radiation Induced Reactions in Polymers Induced Ions

The size of the field depends on
- Reactive intermediates
  - Density
  - Stability
- Linear energy transfer: LET
- Structure of a molecule (Mw, Stiffness, etc.)

Very good size control and mass production

Ion Track Structure in Polysilanes

- Polysilanes
  - » Silicon Analog of Polyethylene
  - » 1-D Analog of Crystalline Si

- Properties
  - Electroluminescence
  - Photoconductivity
  - 1-D Quantum wires
  - Radiation Sensitive

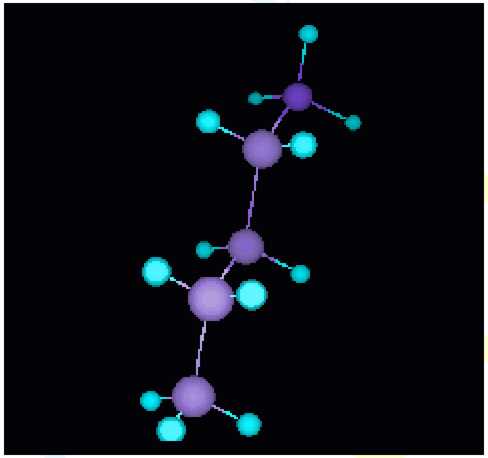

Uniformity of Nano-Wires

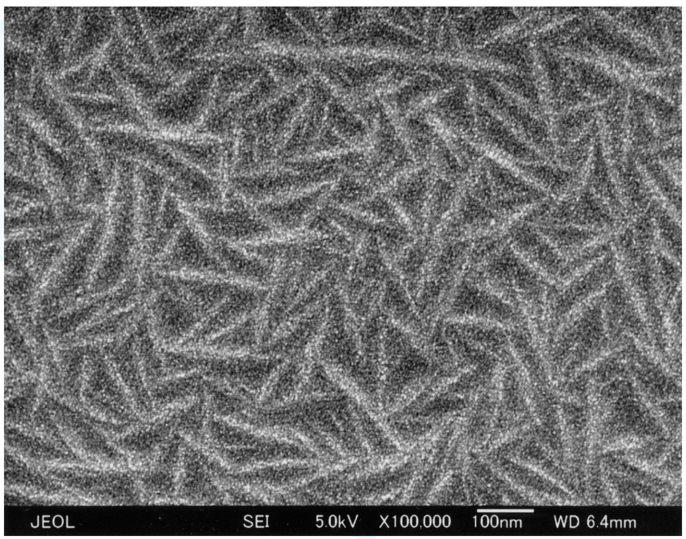

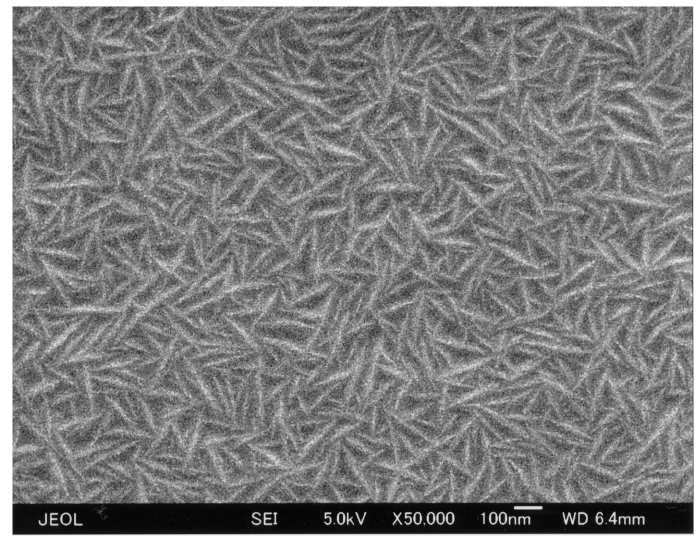

Figure. A SEM image of rod-like nano-wires on a Si substrate. The nano-wires were formed by the 450 MeV $^{128}Xe^{23+}$ irradiation to a **PS3** thin film (200 nm thick) at 1.6 x 10^{12} ions/cm^{2}. The film was developed by hexane, and heated up to 523 K for 0.5 h after irradiation.

Uniform Formation of Nanowires

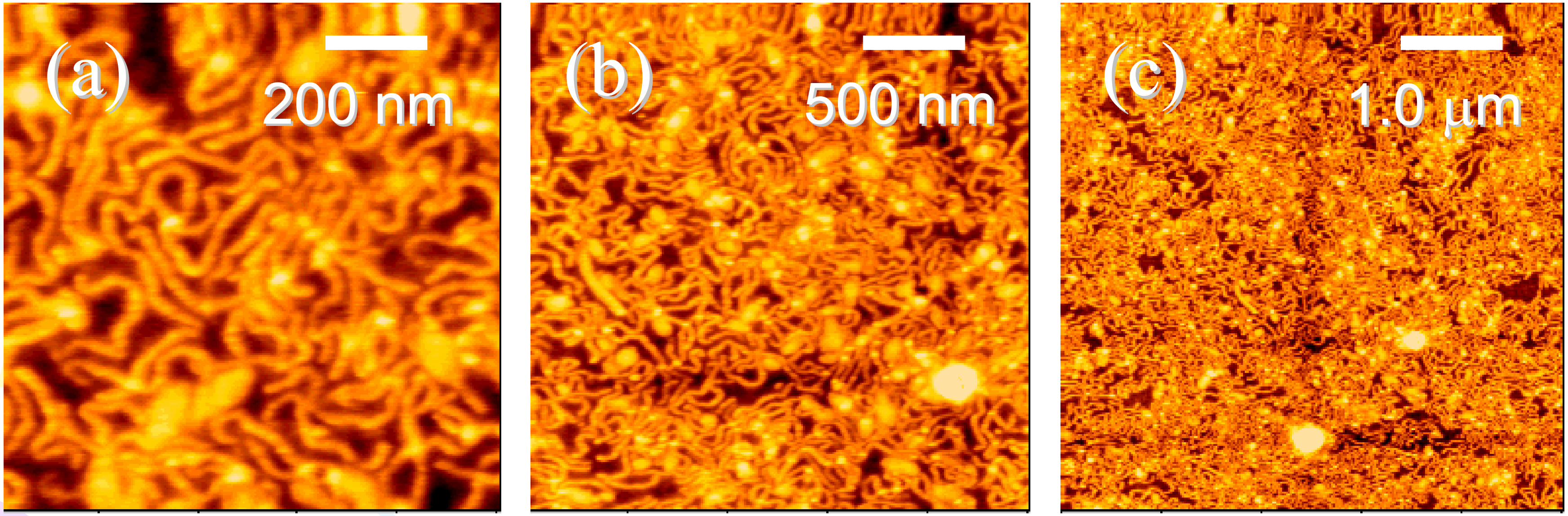

Figure. AFM images of nano-wires on a Si substrate with a variety of special resolutions. The nano-wires were formed by the 450 MeV $^{128}Xe^{23+}$ irradiation to a **PS1** thin film (0.40 mm thick) at 1.7 x 10^{10} ions/cm^2.

ns pulse radiolysis

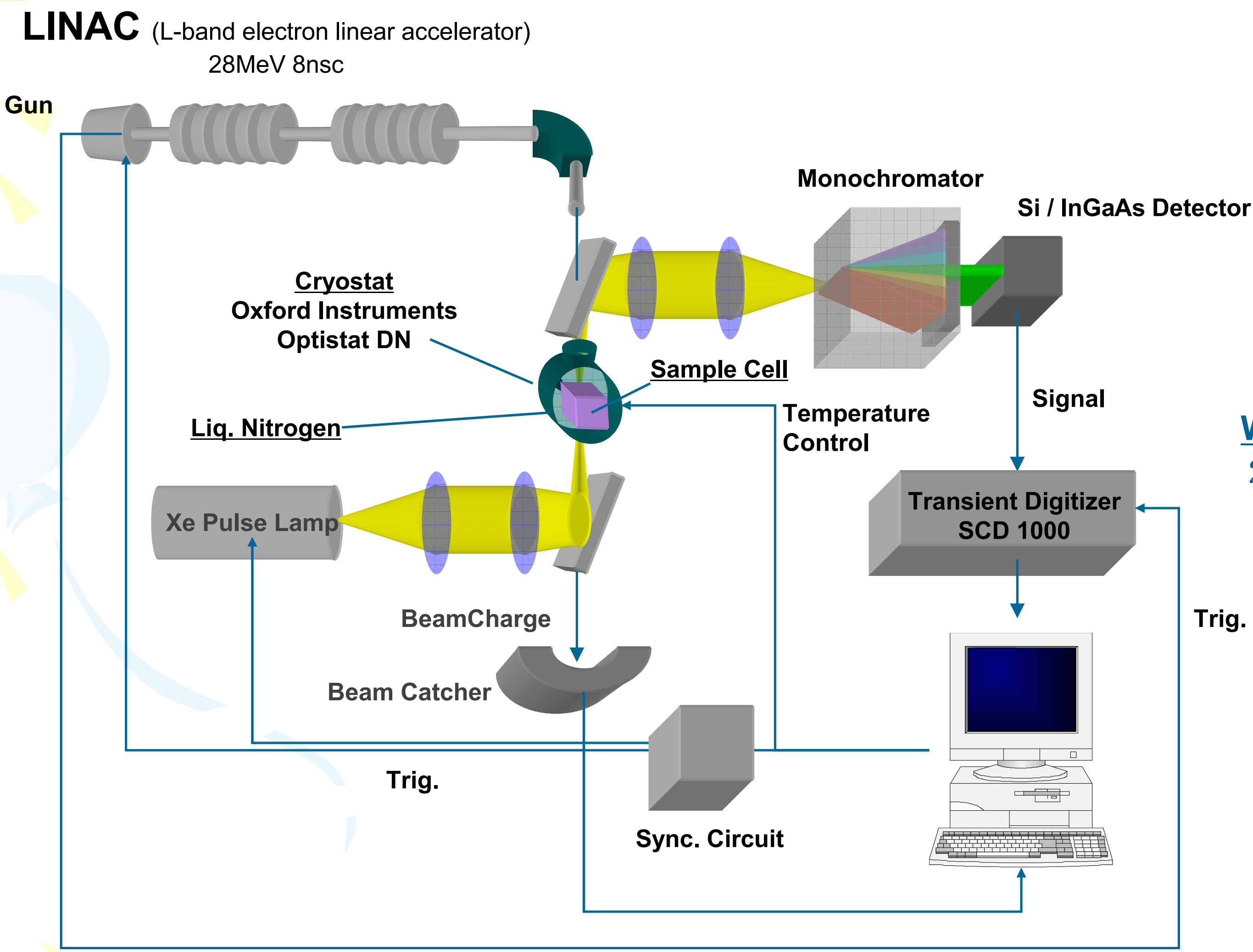

Wavelength Range

２５０ｎｍ～２１００ｎ

ns pulse radiolysis

A kinetic trace in wide dynamic range can be measured by one pulse irradiation

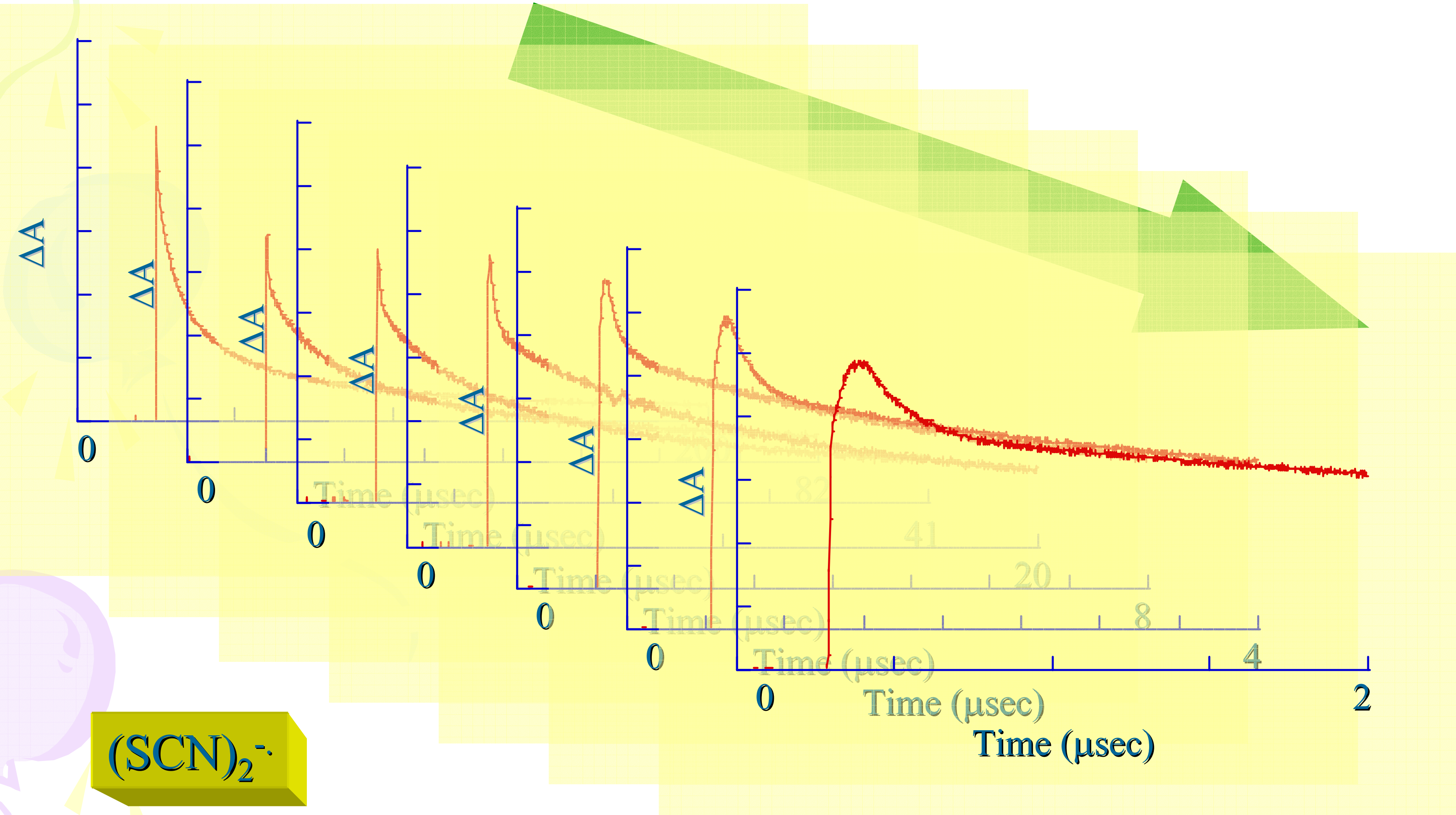

In-situ TRMC-TAS

In-situ TRMC-TAS

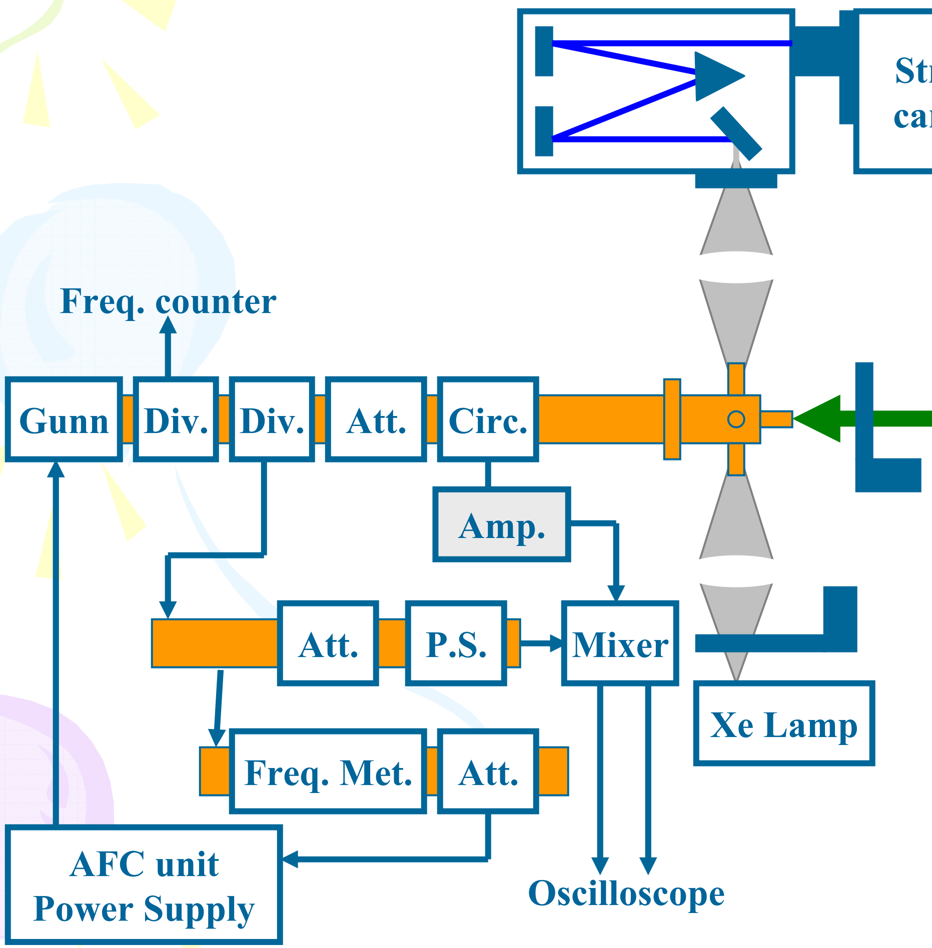

Materials (Film)

Dissolved in THF and drop-casted on quartz substrate.

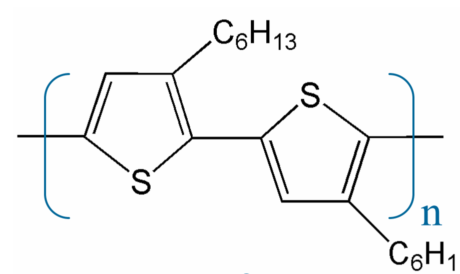

RR-P3HT

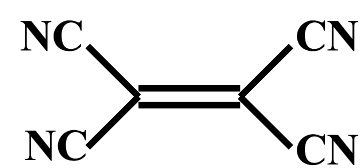

TCNE

History of pulse radiolysis at ISIR

ns system

UV, Vis 1994
NIR, 1995
Low-temp, NIR, Vis, 1997
IR, 1998
UV, Vis, ns-ms, 2001

ps system (stroboscopic)

Laser-linac synchronized, 1995
Vis, 1998
Pulse compression, 1998
Jitter compensation, 1999
Improvement of S/N ratio, 2001

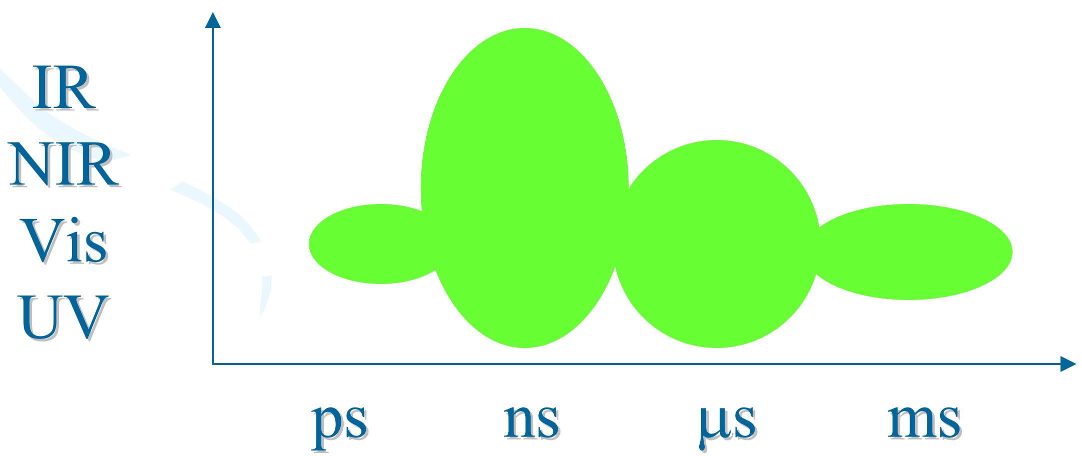

Nanobeam Processes and Development of Nanomaterials

Ultra-fine Electron Beams

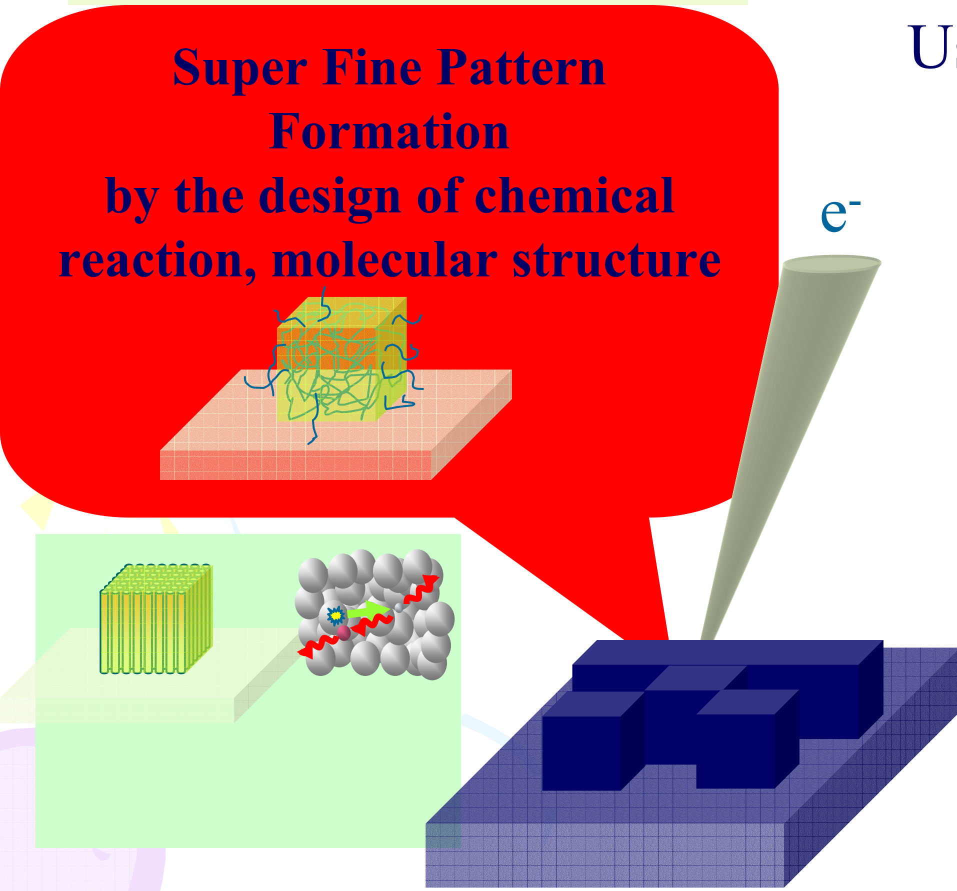

Use of Single Charged Particle Events

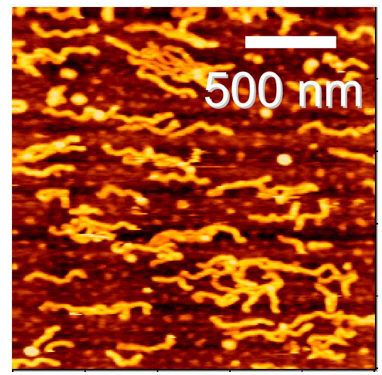

Nano-fluorescent Light

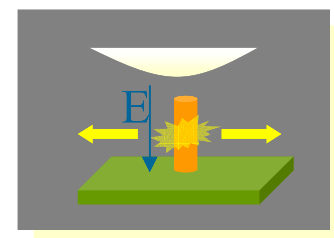

Single Ion Track

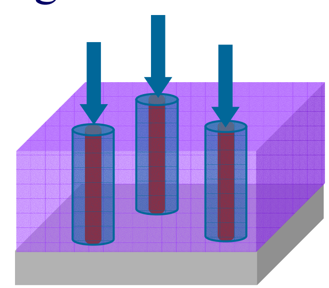

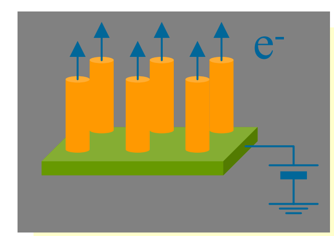

Field Emitter

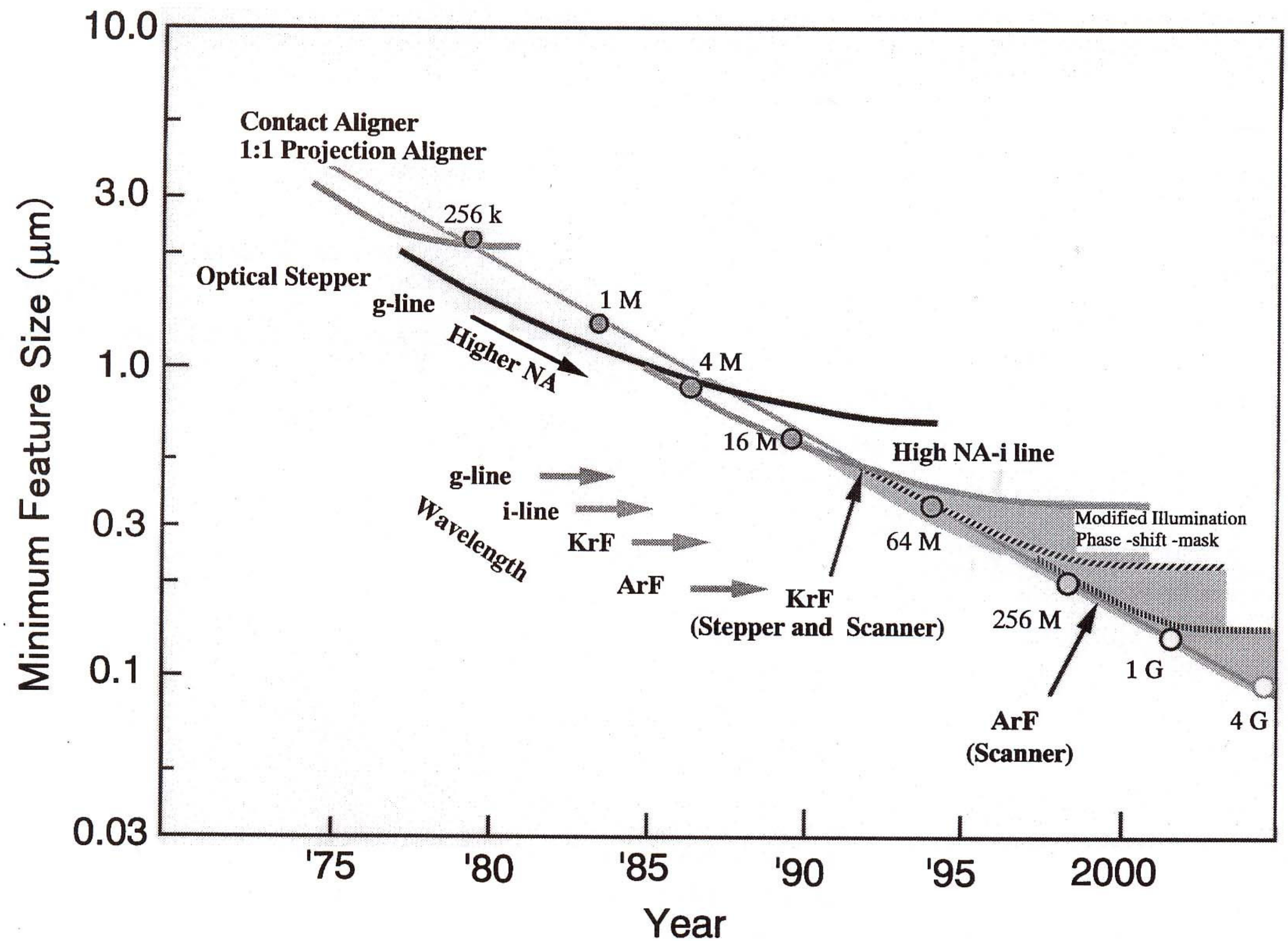

Miniaturization trends of DRAM pattern size and development of optical lithographic tools. DRAM capacity is given in bits.

Sub-Half-Micron Lithography for ULSIs edited by K. Suzuki, S. Matsui and Y. Ochiai

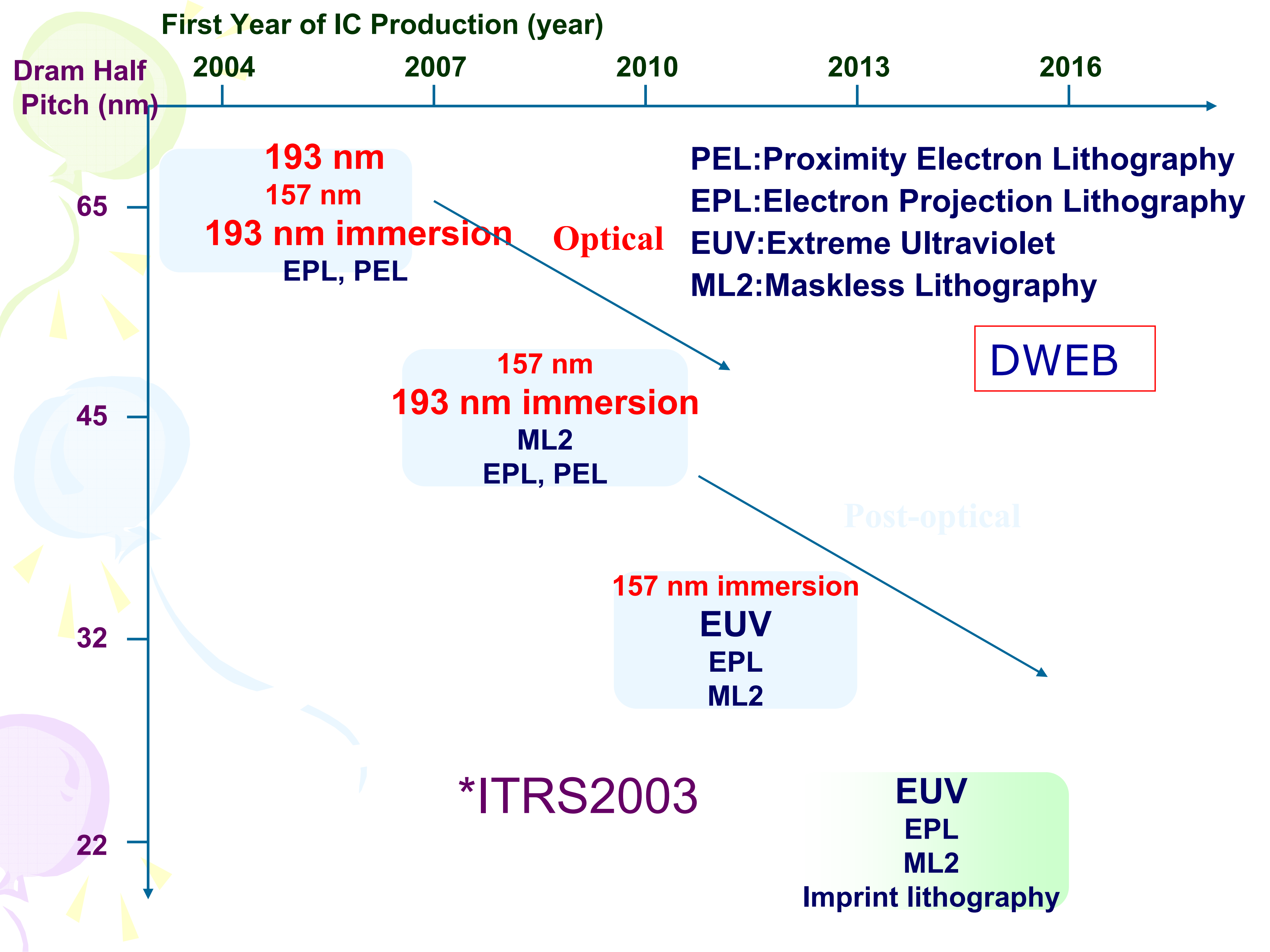
First Year of IC Production (year)
Dram Half Pitch (nm)
2004
2007
2010
2013
2016
65
45
32
22
193 nm
157 nm
193 nm immersion
EPL, PEL
Optical
PEL:Proximity Electron Lithography
EPL:Electron Projection Lithography
EUV:Extreme Ultraviolet
ML2:Maskless Lithography
DWEB
157 nm
193 nm immersion
ML2
EPL, PEL
Post-optical
157 nm immersion
EUV
EPL
ML2
*ITRS2003
EUV
EPL
ML2
Imprint lithography

Table 78a Resist Requirements—Near-term

Year of Production	2003	2004	2005	2006	2007	2008	2009
Technology Node		hp90			hp65		
DRAM ½ Pitch (nm)	100	90	80	70	65	57	50
MPU/ASIC Metal 1 (M1) ½ Pitch (nm)	120	107	95	85	76	67	60
MPU/ASIC ½ Pitch (nm) (un-contacted gate)	107	90	80	70	65	57	50
MPU Gate in resist Length (nm)	65	53	45	40	35	32	28
MPU Gate Length after etch (nm)	45	37	32	28	25	22	20
Resist Characteristics *							
Resist meets requirements for gate resolution and gate CD control (nm, 3 sigma) **	◆ 4.0	3.3	2.9	2.5	2.2	2.0	1.8
Resist thickness (nm, imaging layer) ***	250–400	220–360	200–320	170–250	160–220	140–200	130–180
Ultra thin resist thickness (nm)****	120–150	120–150	120–150	100–150	100–130	100–130	80-120
PEB temperature sensitivity (nm/C)	2.5	2	2	1.5	1.5	1.5	1.5
Backside particles (particles/m^2 at critical size, nm)	2000 @ 150	2000 @ 150	1500 @ 100	1500 @ 100	1500 @ 100	1500 @ 100	1000 @ 50
Defects in spin-coated resist films† #/cm^2	0.02	0.01	0.01	0.01	0.01	0.01	0.01
(size in nm)	60	55	50	45	40	35	30
Defects in patterned resist films, gates, contacts, etc. #/cm^2	0.07	0.06	0.05	0.04	0.04	0.03	0.03
(size in nm)	60	55	50	45	40	35	30
Line Width Roughness (nm, 3 sigma) <8% of CD ******	◆ 3.6	3.0	2.6	2.2	2.0	1.8	1.6

Manufacturable solutions exist, and are being optimized

Manufacturable solutions are known

Interim solutions are known ◆

Manufacturable solutions are NOT known

*ITRS2003

What limits the resolution of EB lithography

The limit of the resolution of the high sensitive EB resists is key problem for the future lithographies (both EB and EUV lithograph).

It is also essence for the development of nanotechnology.

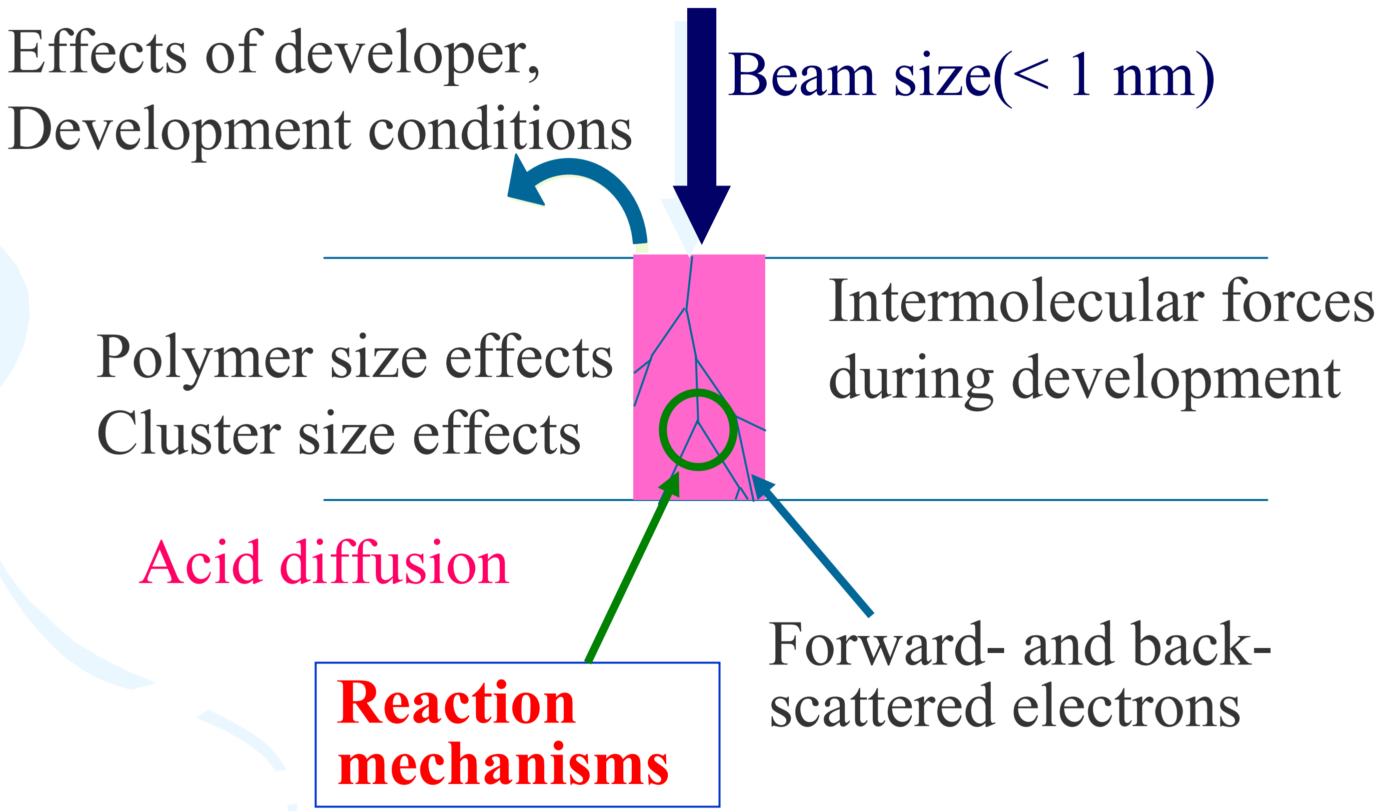

EB can be focused less than 1 nm. However, technical barriers exist around 30-50 nm for mass production type resist pattern. Why?

More important problem is critical dimension (CD) and Line edge roughness (LER).

Chemically amplified resist

Generation of acid by exposure

$$Ph_3S^+X^- \xrightarrow{h\nu\text{、radiation}} H^+X^-$$

Pattern formation utilizing polarity change by deprotection reaction

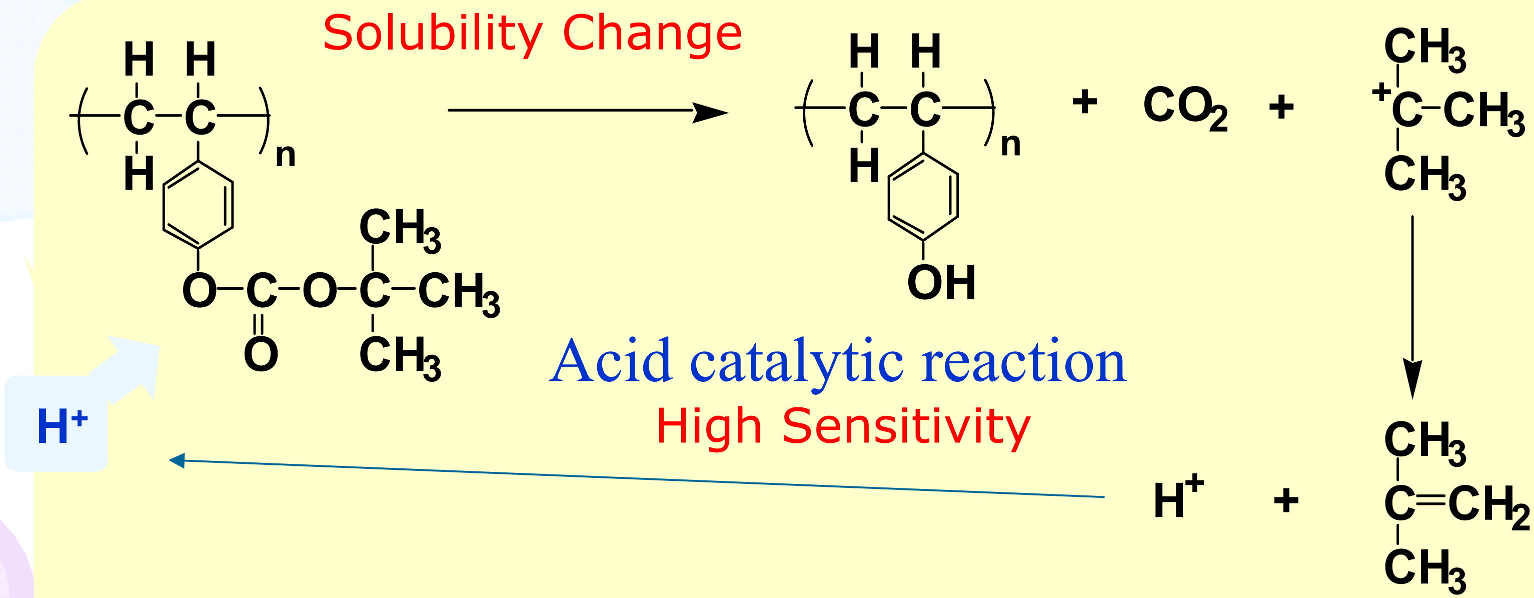

×Polmerization, graft polmerization, and others

Acid generation mechanism – Ionization channel

Electron beam, X-ray, EUV

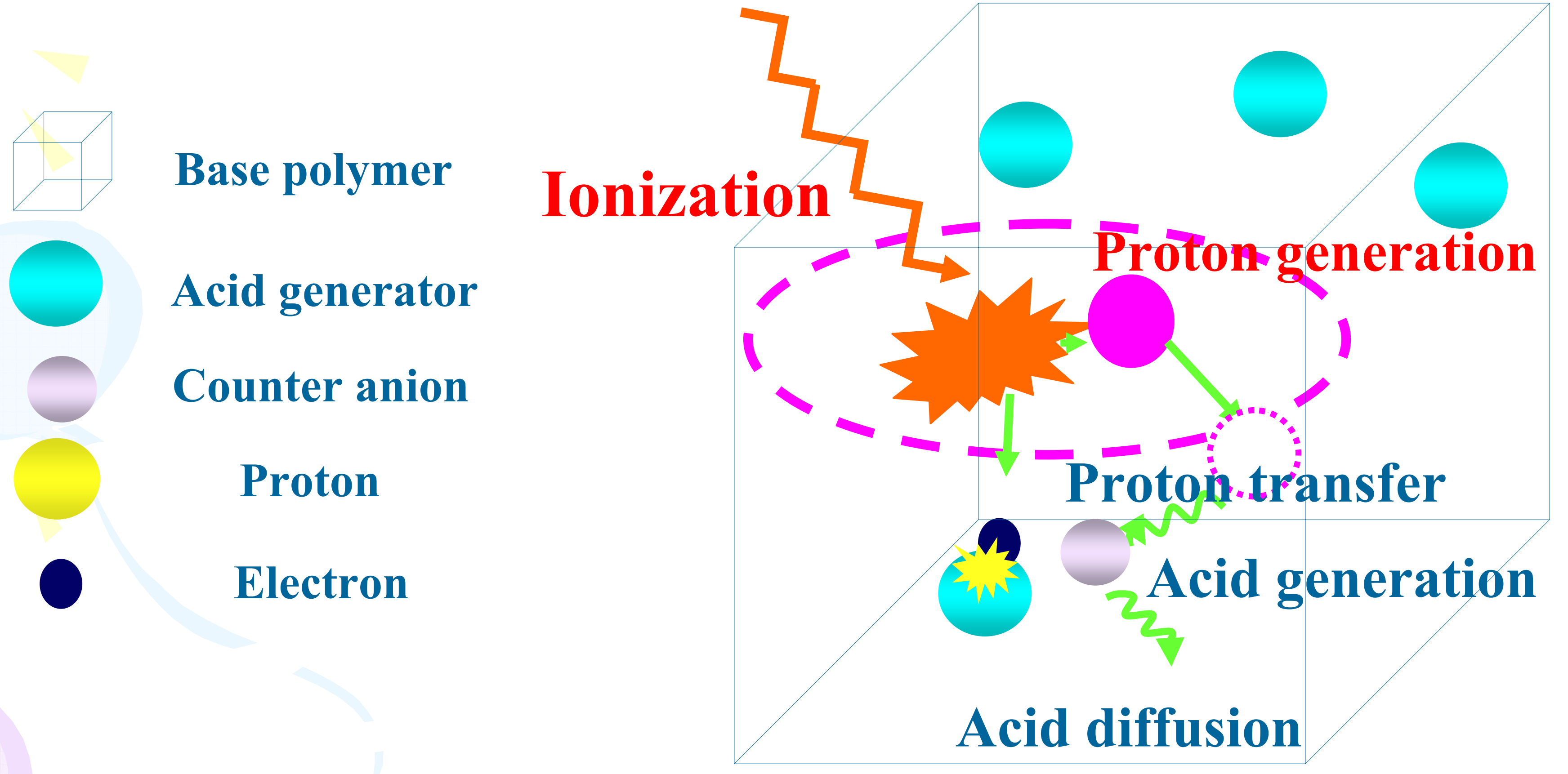

Reaction control in nanospace --Time space translation

A. Saeki et al. Jpn. J. Appl. Phys. 41 (2002) 4213.

It is essential to minimize the displacement between energy deposition point and reaction point.

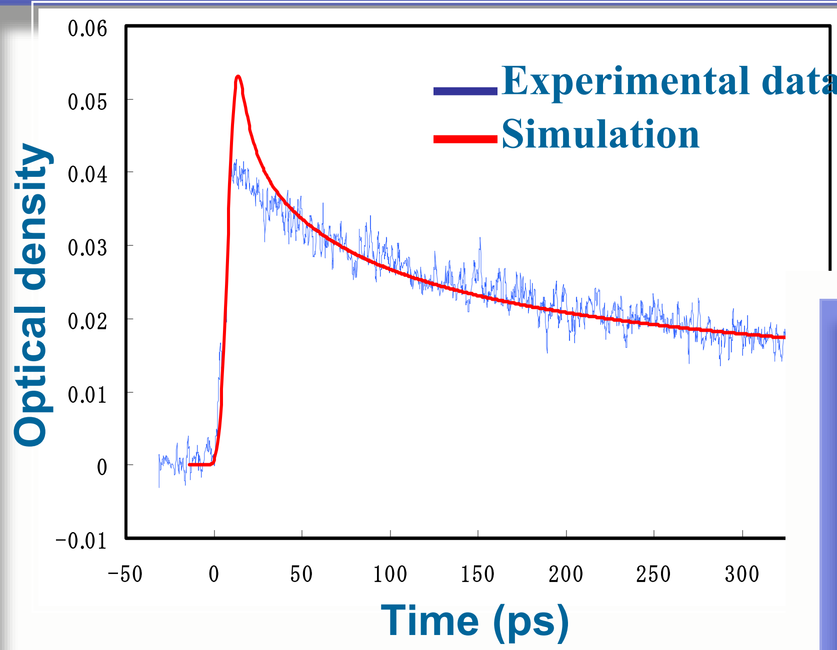

Experimental data obtained in the femtosecond pulse radiolysis and simulation

Time-space translation

Translation of picosecond temporal data to nanometer spatial data

（So far, available only at ISIR）

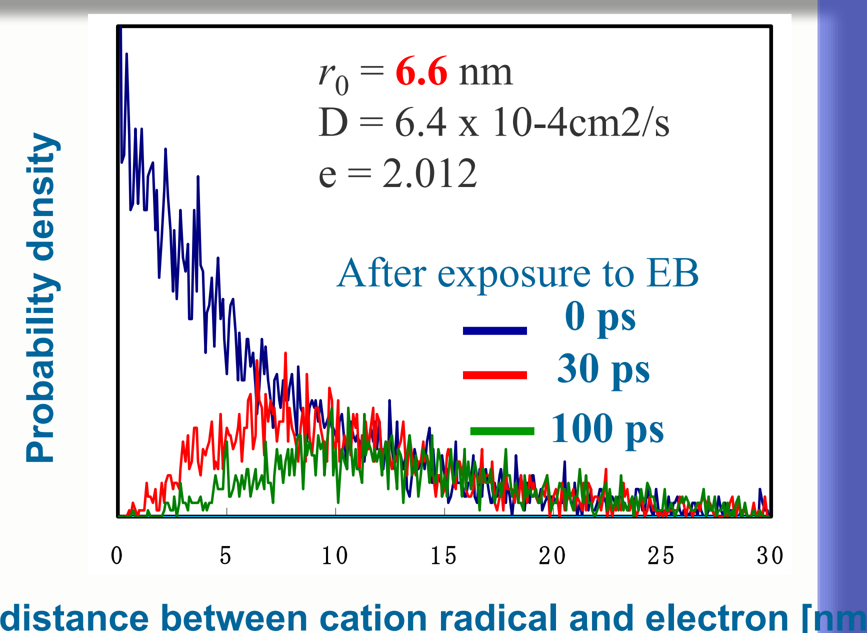

Change of distance between electron and cation radical generated by electron beam irradiation.

Spatial separation between electron and cation radical causes the displacement between energy deposition point and reaction point. For the nanotechnology, it is essential to decrease the displacement.

Electron dynamics in early processes of radiation chemistry

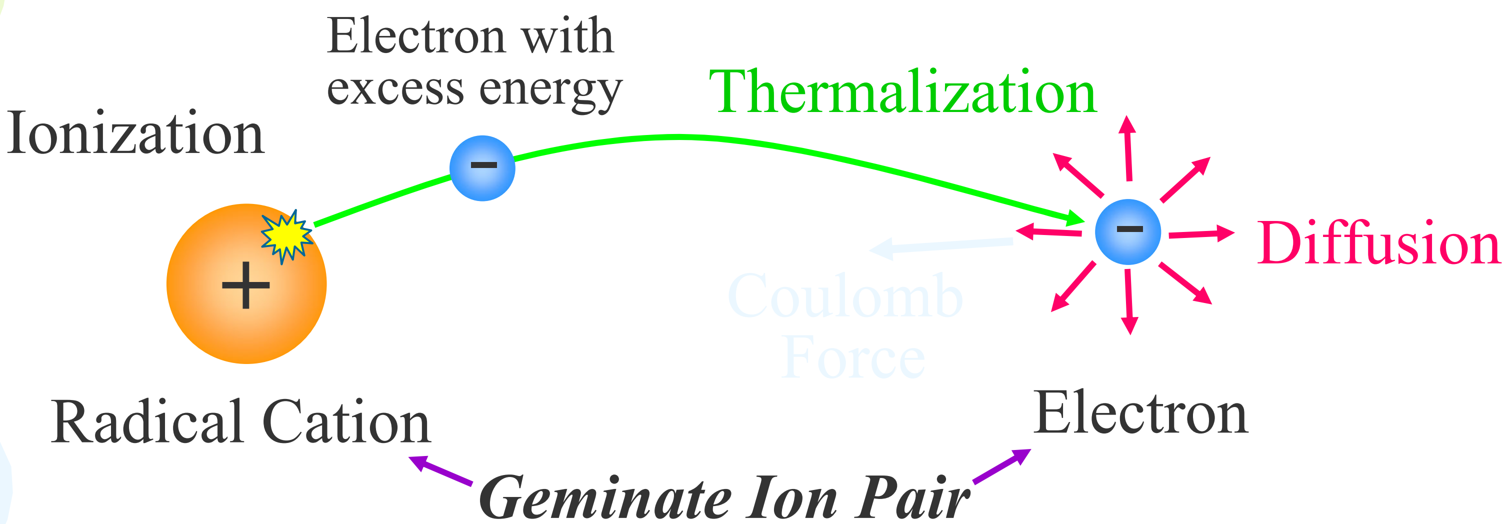

Smoluchowski equation

$$\frac{\partial w}{\partial t} = D\nabla\left(\nabla w + w\frac{1}{k_B T}\nabla V\right)$$

w : Probability density of electrons
$\boldsymbol{k_\mathrm{B}}$: Boltzmann constant
V : Coulomb potential
T : Absolute temperature
D : Sum of diffusion coefficient

Initial distribution function

$$f(r, r_0) = \frac{1}{r_0}\exp\left(-\frac{r}{r_0}\right)$$

r : Distance between radical cation and electron
$\boldsymbol{r_0}$: Initial separation distance on average

n-Dodecane

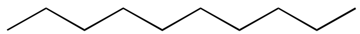

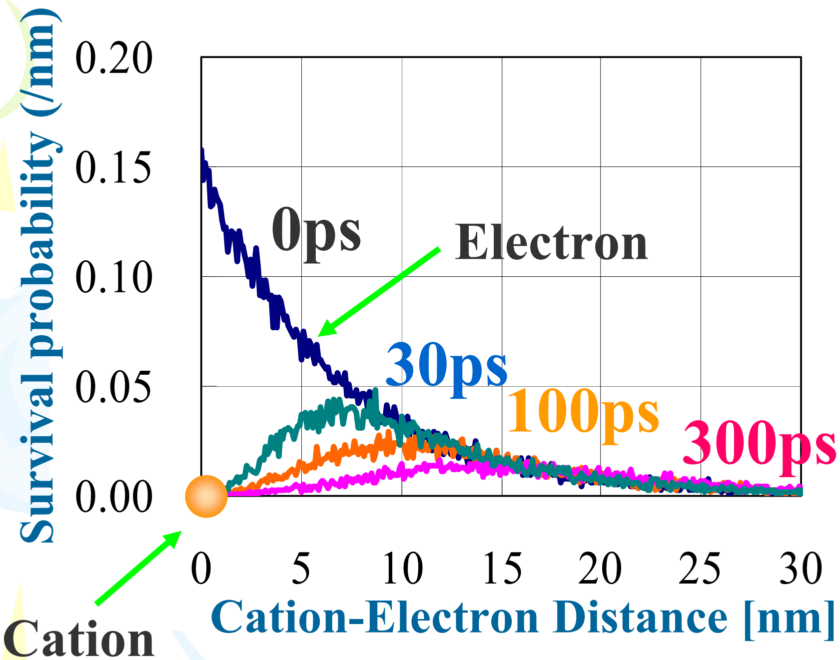

Distribution of Electron

r_0 = **6.6** nm

D = 6.4 x 10^{-4} cm^2/s

ε = 2.012

Benzene

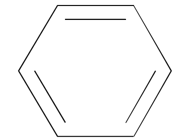

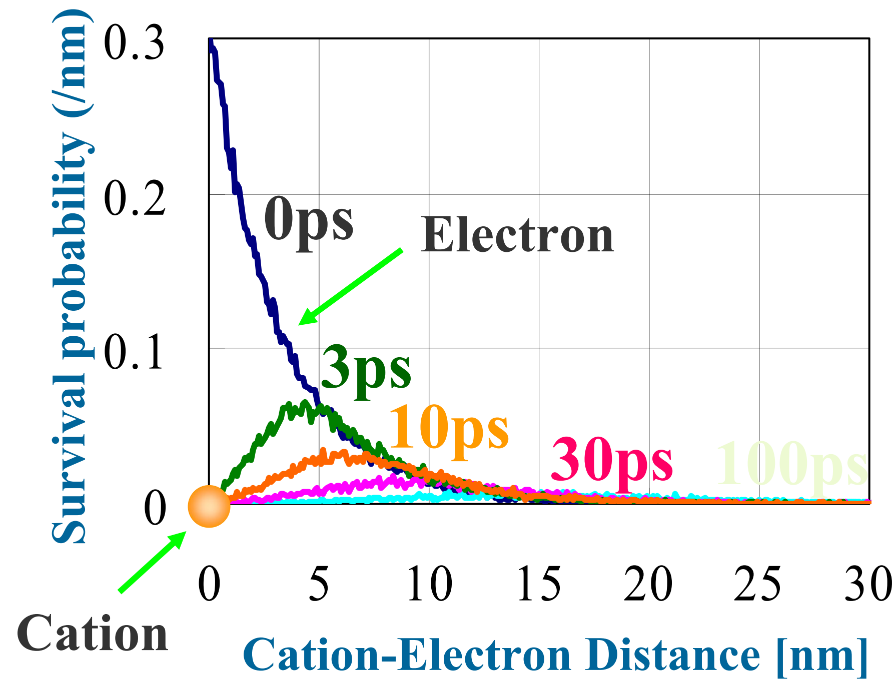

Distribution of Electron

r_0 = **3.2** nm

D = 2.8 x 10^{-3} cm^2/s

ε = 2.284

Base Polymers for Lithographies

g / i	KrF	ArF	F_2
Aromatic ring		Alicyclic groups Cyclic olefine polymer	F polymer
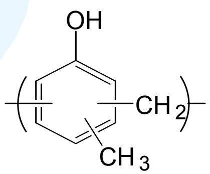 Nobolak resin	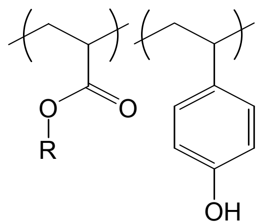 Poly(acrylate -hydroxystyrene) 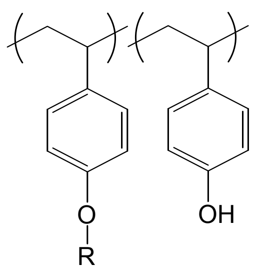 Ploy(p-hydroxystyrene)	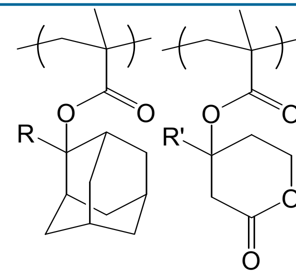 Ploy(methacrylate) 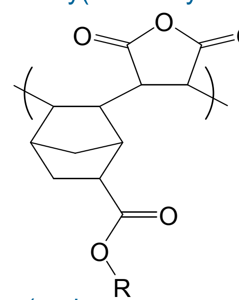 Ploy(norbornene - maleic anhydride) 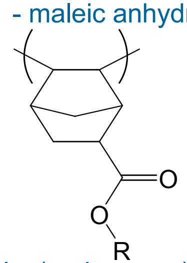 Ploy(norbornene)	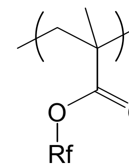 Ploy(methacrylate) 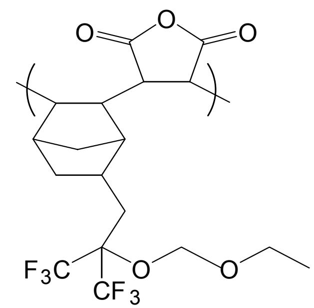 Ploy(norbornene - maleic anhydride) 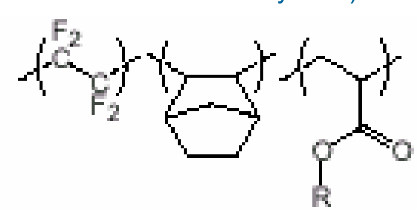 [TFE/NB type]

Acid generation mechanism – Ionization channel

Electron beam, X-ray, EUV

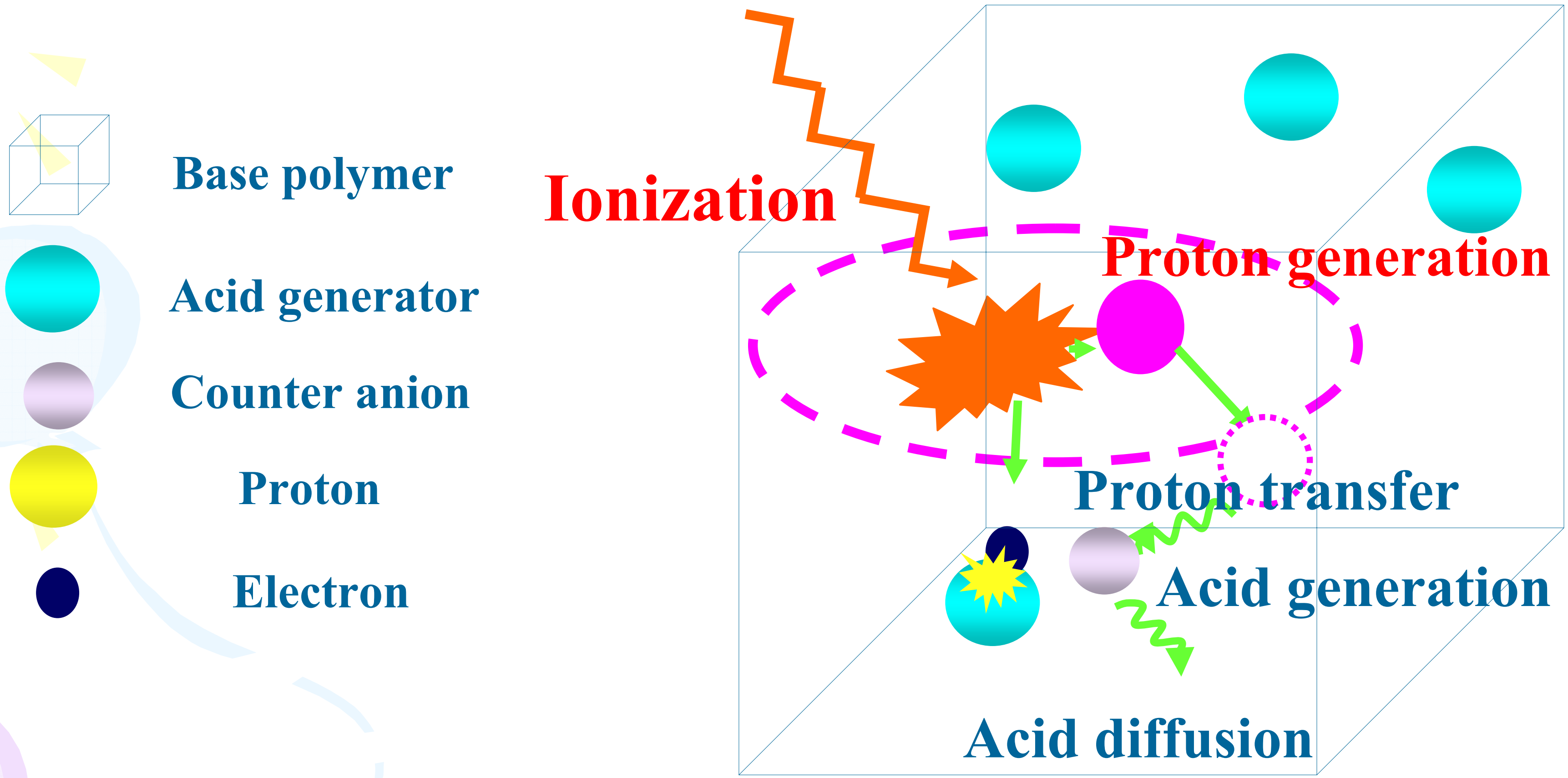

Formulation

The reaction of acid generators with electrons:

$$\frac{\partial w}{\partial t} = -kCw$$

Effective reaction radius of acid generators:

$$k = 4\pi RD$$

Electron dynamics in resist materials:

$$\frac{\partial w}{\partial Dt} = \nabla\left(\nabla w + w\frac{1}{k_B T}\nabla V\right) - 4\pi RCw$$

w : probability density of electrons
k : rate constant of reaction of acid generator with electrons
C : concentration of acid generators
R : effective reaction radius

Effective reaction radii of acid generators

Acid generator	k ($M^{-1}s^{-1}$)	R (nm)	Acid generator	k ($M^{-1}s^{-1}$)	R (nm)
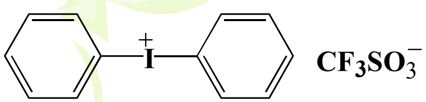	2.4×10^{10}	**2.1**	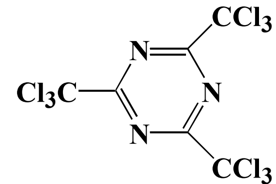	2.2×10^{10}	**1.9**
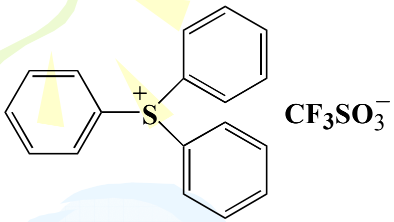	2.7×10^{10}	**2.4**	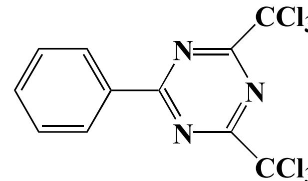	2.5×10^{10}	**2.2**
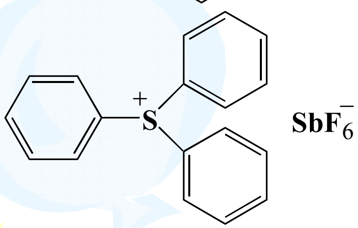	2.5×10^{10}	**2.2**	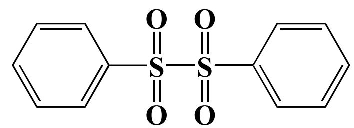	1.1×10^{10}	**0.96**
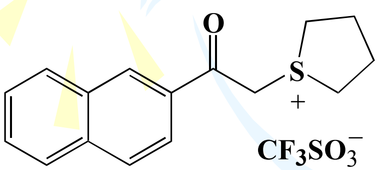	1.9×10^{10}	**1.7**	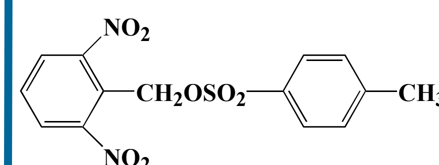	2.2×10^{10}	**1.9**
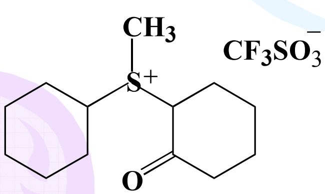	1.6×10^{10}	**1.4**			

$$k = 4\pi RD$$

R : Effective reaction radius of acid generators

D : Diffusion coefficient of solvated electrons in methanol (1.5×10^{-9} m^2s^{-1})

k : Rate constant of reaction of acid generators with solvated electron in methanol

Distribution change of electrons around ionization point

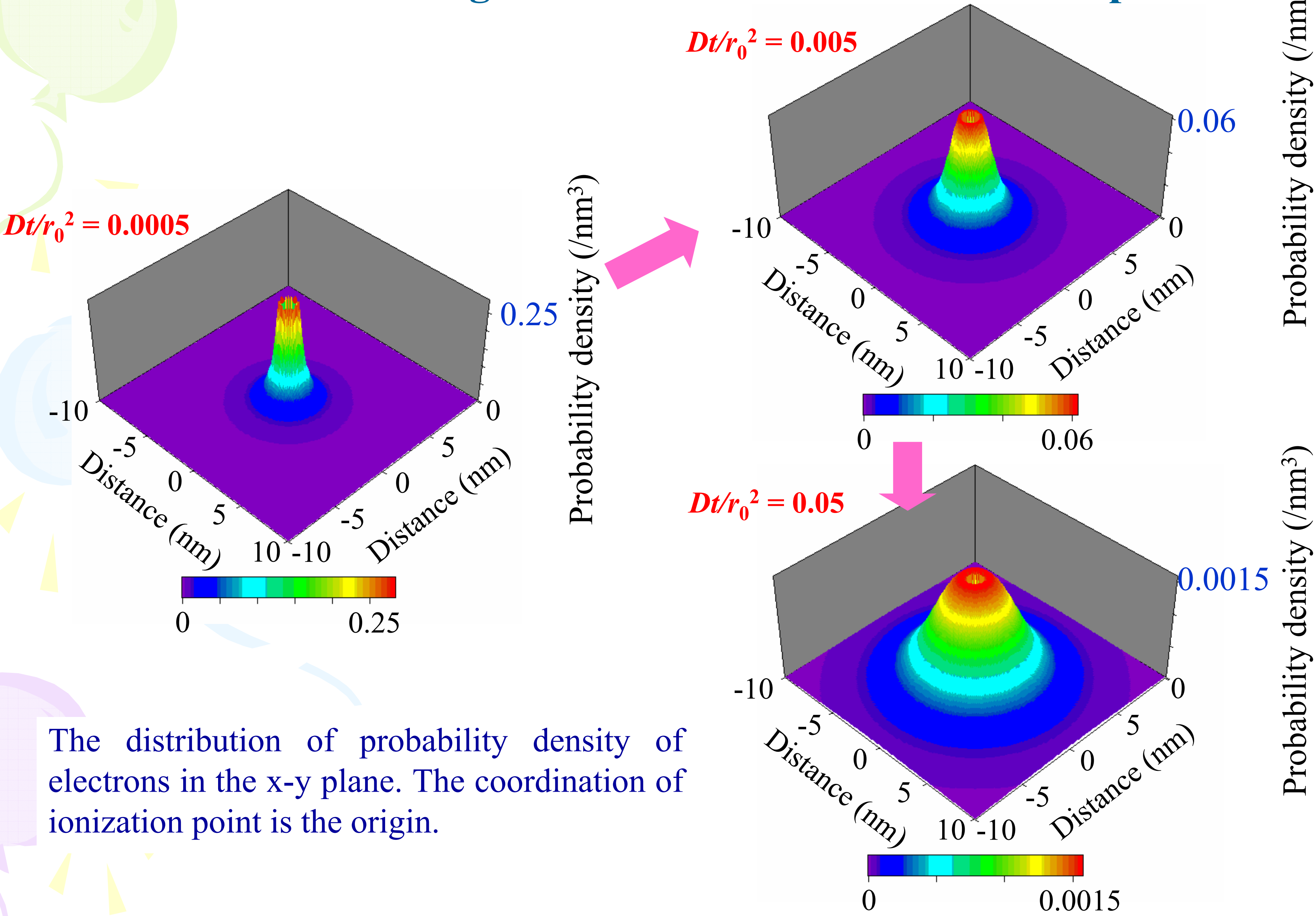

The distribution of probability density of electrons in the x-y plane. The coordination of ionization point is the origin.

Counter anion distribution around ionization point

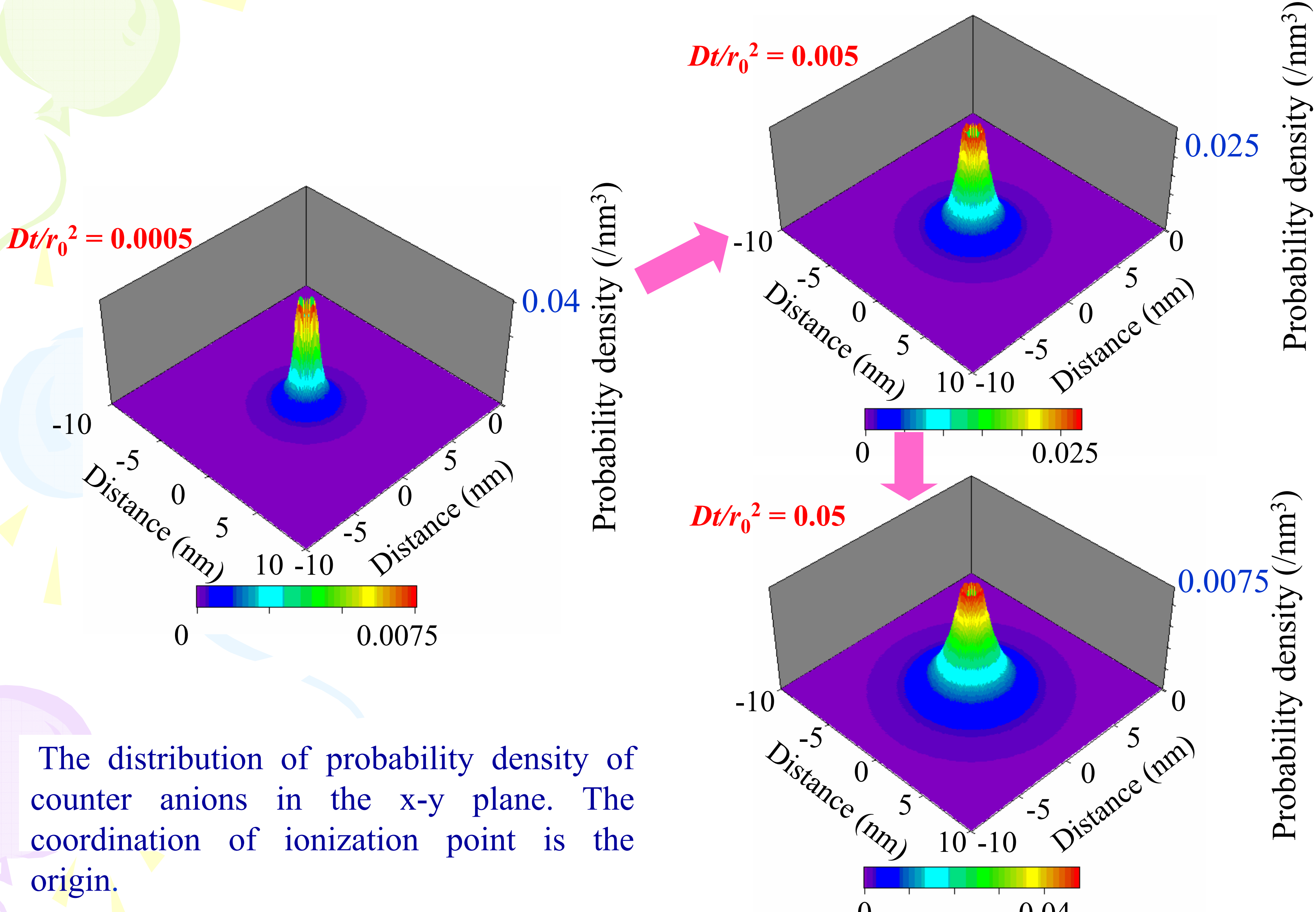

The distribution of probability density of counter anions in the x-y plane. The coordination of ionization point is the origin.

Conclusion 2

The elucidation of the reaction mechanisms of chemically amplified resists is very important in the development of the resists with at least both high sensitivity and high space resolution. Our findings were integrated to a simulation model. This model is applicable to exposure souses whish have higher energy than ionization potential of resist materials. The probability density of acid distribution around ionization point was simulated with a typical parameter set.